LAWRENCE
LIVERMORE
NATIONAL
LABORATORY

UCRL-CONF-221544

# Scrape-Off Layer Plasmas for ITER with 2nd X-Point and Convective Transport Effects

T.D. Rognlien, R.H. Bulmer, M.E. Rensink, J.N. Brooks

May 22, 2006

17th International Conf. on Plasma Surface Interactions in Controlled Fusion Devices
Hefei, China
May 22, 2006 through May 26, 2006

**Disclaimer**

This document was prepared as an account of work sponsored by an agency of the United States Government. Neither the United States Government nor the University of California nor any of their employees, makes any warranty, express or implied, or assumes any legal liability or responsibility for the accuracy, completeness, or usefulness of any information, apparatus, product, or process disclosed, or represents that its use would not infringe privately owned rights. Reference herein to any specific commercial product, process, or service by trade name, trademark, manufacturer, or otherwise, does not necessarily constitute or imply its endorsement, recommendation, or favoring by the United States Government or the University of California. The views and opinions of authors expressed herein do not necessarily state or reflect those of the United States Government or the University of California, and shall not be used for advertising or product endorsement purposes.

# Scrape-off layer plasmas for ITER with $2^{nd}$ X-point and convective transport effects

T.D. Rognlien[1], R.H. Bulmer[1], M.E. Rensink[1], and J.N. Brooks[2]

[1] *Lawrence Livermore National Laboratory, Livermore, CA 94551 USA*
[2] *Argonne National Laboratory, Argonne, IL 60439 USA*

**Abstract**

Plasma fluxes to the divertor region in ITER near the magnetic separatrix have been modeled extensively in the past. The smaller, but potentially very important fluxes to the main chamber and outer divertor regions are the focus of the present paper. Two main additions to the usual transport modeling are investigated: namely, convective radial transport from intermittent, rapidly propagating "blob" events, and inclusion of the magnetic flux-surface region beyond the second X-point that actually contacts the main-chamber wall. The two-dimensional fluid transport code UEDGE is use to model the plasma, while the energy spectrum of charge-exchange neutrals to the main chamber wall is calculated by DEGAS 2 Monte Carlo code. Additionally, the spatial distribution of Be sputtered from the main chamber wall is determined in the fluid limit.

JNM Keywords: Plasma-Material Interaction (P0500), Plasma Properties (P0600), Theory and Modeling (T0100), First wall materials (F0400)

PSI-17 Keywords: edge transport, divertor modelling, Impurity transport, non-diffusive transport, first wall, Beryllium, UEDGE, DEGAS

PACS: 52.40.Hf, 52.25.Fi, 52.55.Rk, 52.65-y, 52.25.Vy

Corresponding/Presenting Author:
Thomas D. Rognlien
P.0. Box 808, L-630
7000 East Ave
Livermore, CA 94550 USA
E-mail: trognlien@LLNL.GOV

## 1 Introduction

The scrape-off layer (SOL) plasma characteristics are key is determining plasma fluxes to material surfaces that determine peak heat loads, material lifetime, and hydrogenic and impurity particle sources via recycling and sputtering. Because of the mixed-material aspect to the ITER wall [1] (mostly Be and with W above the divertor region) and the divertor plates (C), it is especially important to model plasma fluxes to these specific areas and to determine the intermixing of materials owing to spatial transport and re-deposition of sputtering materials.

Two new aspects of divertor physics for ITER are analyzed in this paper: first, the effect of possible strong radial convection of SOL plasma to the main chamber wall and the resulting Be sputtering, and second, the inclusion of the outer SOL on magnetic flux-surfaces beyond the secondary X-point. The study thus provides an extension of the previous 2D plasma transport modeling where both effects were ignored, *e.g.*, [2]. Because the turbulent transport of hydrogen and impurities in the outer SOL of ITER is not well characterized, the present analysis simply provides plausible estimates based on experimental data from present-day devices, and thus gives a measure of the potential importance of the two new aspects modeled. Rapid convective transport of plasma in the SOL has been observed or inferred by various diagnostics, such as Langmuir probes, Gas-Puff imaging, and imaging of background $H_\alpha$ light ( [3–5] and references therein). Analysis of polarization of plasma density "blobs" from opposite ion and electron $\nabla B$ drifts, and the resulting $\mathbf{E} \times \mathbf{B}$ drift, provides a simple explanation of the rapid outward motion [6]. Analysis of data from Alcator C-Mod and DIII-D tokamaks indicate that the time-averaged radial convective velocity can reach 100 m/s or more, and appears to increase with edge density [5]. Likewise, coupled turbulence/transport simulations show time-averaged velocities in this range for DIII-D parameters [7]. The ubiquitous nature of such convection and just how it depends on operating modes is not well understood, but the effect seems stronger at higher densities approaching the Greenwald limit, which is where ITER will operate. In both experiments and simulations, the time-averaged radial velocity is much less than the peak radial velocity owing to the strongly intermittent nature of the turbulence. The impact of convective SOL edge-plasma transport has been analyzed previously for other devices [8,9].

As designed, there can be some significant radial distance between the ITER wall and the secondary separatrix determined by the magnetic flux surface intersecting the second magnetic X-point at the top of ITER. The hydrogenic plasma striking the separate Be and W portions of the wall will be in this outer SOL region, the structure of which has been omitted in previous 2D plasma transport modeling, The 2D UEDGE transport code [10] now includes

the ability to simulate extended SOL plasmas with both primary lower X-point adjacent to the core region and the secondary upper X-point and the radial domain sometimes reference to as the far SOL. The charge-exchange neutral hydrogen flux to the wall is assessed with the DEGAS 2 Monte Carlo neutral code [11]. The impurity level in the edge plasma and the spatially dependent redeposition fluxes of different impurities are modeled from the multi-component fluid model using approximate sputtering rates. The sensitivity of the impurities results to different convective transport models for each impurity charge state is shown.

The paper presents the geometry and simulation models in Sec. 2, gives results for the hydrogenic plasma in Sec. 3, Be sputtering and transport in Sec. 4 and provides a discussion and summary in Sec. 5.

## 2 Geometry and simulation models

The ITER geometry used is shown in Fig. 1, where the interior lines all correspond to poloidal magnetic flux surfaces taken from an MHD equilibrium for ITER midway through its discharge. The dotted (red) line shows the primary separatrix adjacent to the core region and the dashed (green) line is the secondary separatrix associated with the X-point at the top of the device. Previous transport modeling of ITER has taken the main chamber wall to be slightly inside the secondary separatrix to allow single-null simulations. However, as can be seen in Fig. 1, a substantial radial region (far SOL) exists between the secondary separatrix and the actual ITER wall. Our extended simulations include the region out to the solid line just inside the outer wall, and thus directly encompass the lower tungsten (W) baffle noted in Fig. 1 and a portion of the upper wall where B-field lines intersect the wall.

The model for the edge plasma is taken from the strongly magnetized fluid equations of Braginskii [12] with some reductions as described in Ref. [10]. The 2D mesh is based on magnetic flux surfaces. The turbulence code includes a segment of the toroidal dimension. UEDGE evolves moment equations for the plasma and neutral densities ($n_{i,n}$), parallel ion and neutral fluid momenta ($mn_{i,n}v_{\|i,n}$), and separate electron and ion energy densities ($3n_{e,i}T_{e,i}/2$). The electrostatic potential ($\phi$) comes from the inertialess parallel electron momentum equation. For the simulations, the radial plasma fluxes are expressed in the form (here for density)

$$\Gamma = -D\nabla_r n + V_c n \tag{1}$$

where $D$ and $V_c$ are specified functions of distance normal to the magnetic flux surface, $\nabla_r$ is the normal derivative, and similar flux relations apply to

the other variables [10]. In the present modeling, classical cross-field drifts are ignored.

For the self-consistent transport simulations, the neutrals of described by a flux-limit fluid model, which gives reasonable neutral source profiles when compared to DEGAS 2 modeling. However to evaluate the energy spectrum of the charge-exchange neutrals incident on the wall, DEGAS 2 [11] is used in a post-processing mode since such information is not available from a fluid model.

## 3 Results for the hydogenic edge plasma

The base-case for ITER used here has 100 MW injected from the core into the edge region, split equally between ions and electrons. The anomalous radial diffusion coefficients at $D = 0.3$ m$^2$/s for density and $\chi_{e,i} = 1$ m$^2$/s for electron and ion temperatures as well as perpendicular viscosity for $v_\parallel$. A simplified fixed-fraction carbon impurity model is used with 3% carbon in coronal equilibrium; multi-species carbon produces similar results. The divertor and wall recycling coefficients are set to unity. For the standard edge domain treating only the single-null portion of the edge, we obtain on the outer divertor a peak particle power flux of 5 MW/m$^2$ where the radiation flux is 7 MW/m$^2$ due largely to the 53% of the input power radiated by the carbon. These results are similar to the partially-detached operating mode of ITER [2].

To model the case with convection, we assume a nearly exponentially increasing $V$ for the density, *i.e.*,

$$V_c(r) = V_1 \exp(-r/r_v) + C_1 \tag{2}$$

with a maximum of 70 m/s at the wall where the poloidal flux is $\psi_{max} = 1.035$ (with $\psi = 1$ on the primary separatrix), $r_v = 0.027$ m, and $C_1 = -1.4$ m/s. To model the ballooning nature of the turbulence, the convection is only applied to the outer half of the torus between the upper and lower X-points, except for the 0.5 m poloidal region closest to the X-points. The magnitude and profile of $V_c$ is in the range deduced from C-Mod and DIII-D data [5] and simulations of DIII-D edge turbulence [7].

The base-case ITER simulation is repeated with the addition of $V_c$, and the results are shown in Figs. 2 and 3. In Fig. 2a, one sees the radial ion velocity at the midplane now having both convective and diffusive ($V_D = -D\nabla_r n_i/n_i$) components. For the base-case with $V_c = 0$, $V_D$ is similar in the core, and rises to about 20 m/s half-way into the SOL before decreasing. The ion density profile is shown in Fig. 2b comparing the base-case and finite-$V_c$ case. The

largest difference is the higher SOL density with $V_c$, which is in turn largely the result of wall recycling producing a strong ionization source in the SOL. The neutral density is plotted in Fig. 3a shown the very strong increase in the density when $V_c$ is used. The increase in ion density coupled with the large $V_c$ at the wall gives a strong ion flux to the wall, shown in Fig. 3b. This flux can give substantial sputtering of Be from the wall, as show in Sec. 4. With this specific choice for $V_c$, the total peak heat flux on the outer plate is 9.7 MW/m$^2$, while that to the inner plate increases.

Next, the region beyond the secondary separatrix, defined by the flux surface passing through the upper X-point in Fig. 1, is included. Here, we utilize UEDGE's unbalanced double null capability. The wall region in the vicinity of the upper X-point behaves like another divertor region with B-field lines intersecting the wall, and the W baffle region in the lower divertor is included explicitly as the extended region of the lower divertor plate. The constant transport diffusion coefficients are the same as in other regions, and the convective velocity $V_c$, when activated, remains constant at is previous wall value of 70 m/s throughout the extended outer midplane region.

The resulting plasma density and electron temperature ($T_e$) are compared in Fig. 4 for the cases with $V_c$ from Eq. 2 and that with $V_c = 0$. In both cases, the density near the second separatrix decreases about a factor of two from the $\psi_{max} = 1.035$ case owing to ions allowed to transport into the far SOL region. Likewise the temperatures decrease by a factor of 1.5. In the far SOL, $T_i$ is about twice $T_e$ for finite $V_c$. The power flow across the secondary separatrix on the outside of the torus is 15 MW for finite $V_c$, and 6 MW for $V_c = 0$, compared to 100 MW injected across the core boundary. The particle flux reaching the new outer wall is reduced by a factor of 2-3 compared to the $\psi_{max} = 1.035$ case, with a large fraction of the difference flowing to the lower W baffle region that is assume not to sputtering owing to the low $(T_e, T_i) \sim (5, 10)$ eV there. The peak heat flux on the outer divertor is about the same as the $\psi_{max} = 1.035$ case for the $V_c = 0$, but increases to $\sim$ 20 MW/m$^2$ for the finite $V_c$ case owing to a large increase in $T_e$ very near the primary strike point. Thus, the partially detached solution can be sensitive to $V_c$ (and also moderate changes in its profile).

## 4 Be sputtering and transport

One of the consequences of possible strong convective transport in the SOL of ITER is sputtering wall material. Here we calculate the impact for finite $V_c$ case using a multi-species Be simulation with UEDGE where the Be source is from wall-sputtered neutrals. Here Be is treated as a trace impurity with the hydrogenic plasma fixed at the profiles described in Sec. 3. The sputtered flux

is taken from the incident hydrogen flux assuming an incident energy of $2T_i + 3T_e$, and is computed from a Be yield curve. In addition to ion sputtering of Be, charge-exchange (CX) neutrals from recycled hydrogen can also sputter. The CX source is evaluated by DEGAS 2 [11] to obtain the full kinetic distribution. The procedure gives that the CX sputtering is a factor of 3-4 smaller than the ion sputtering and will make only a modest correction to the ion sputtering results.

The midplane Be density resulting from the ion sputtering is shown Fig. 5a for two models of $V_c$ for Be. The Be recycling coefficient is set to a negligibly small value of 0.01 on all surfaces. The solid line has $V_c = 0$, and the second assumes that low charge-states (on the periphery) are convected inwards and higher charges-states are convected outward with the hydrogen [8]; simple edge turbulence simulations show impurities being convected inward [9] For the latter case, the convective velocities for charge-states (1, 2, 3, 4) are $(-V_c, -V_c/3, V_c/3, V_c)$. The largest difference between the two solutions is near the primary separatrix and the core, but even the $V_c = 0$ case has 0.67% Be in the core, which should be easily tolerable. The Be can also coat the carbon divertor plate and tungsten baffle, and the Be fluxes to those surfaces are shown in Fig. 5b. Note that the divertor flux between the two $V_c$ models are almost indistinguishable, likely because $V_c$ is always zero in the divertor legs, and the Be path to this region is in the divertor region. For the case $V_c = 0$, the ion sputtering of Be is smaller by orders of magnitude, and the CX sputtering would also be small.

## 5 Summary

The edge-plasma in ITER has been analyzed for an assessment of two new effects, possible strong radial convective transport and the presence of the extended SOL outside the secondary separatrix. We find that these effects are potentially very important for predicting plasma-wall interactions in ITER. However, more detailed and systematic studies are required to draw final conclusions as various elements of the model are uncertain, especially the actual nature of the turbulent transport. This study has shown the following: (1), strong convective transport can result in significant sputtering of Be from the chamber walls, yielding concentration at the core boundary up to 0.67% and significant Be fluxes to the divertor regions; (2), inclusion of the secondary SOL reduces the hydrogen flux to the wall by $\sim 1/3$, partially diverting it to the baffle and "upper divertor" region for this averaged model of convective transport (see next paragraph); and (3), even the primary SOL and peak heat flux to the divertors can be sensitive to details of the $V_c$ profile, even for the same overall peak magnitude.

Finally, we note that conclusion (2) just above may change when the time-dependent blob transport is include since the $V_c$ used is an average value, whereas experiments and theory show that the peak $V_c$ is much larger, but only occurs a small fraction of the time. This larger $V_c$ should preferentially throw more plasma to the chamber wall before it can travel to the lower or upper divertors. This study is underway.

## Acknowledgments

We thank S.I. Krasheninnikov for suggestions related to time-dependent "blob" transport. This work was performed under the auspices of the U.S. Dept. of Energy by the University of California Lawrence Livermore National Laboratory under contract No. W-7405-Eng-48.

## References

[1] M. Shimada, A.E. Costly, G. Federici et al., J. Nucl. Mater. **337-339** (2005) 808.

[2] A.S. Kukushkin, H.D. Pacher, D. Coster *et al.*, Nucl. Fusion **43** (2003) 716.

[3] B. LaBombard, M.V. Umansky, R.L. Boivin *et al.*, Nucl. Fusion **40** (2000) 2041.

[4] J.A. Boedo, D.L. Rudakov, R.A. Moyer *et al.*, Phys. Plasmas **10** (2003) 1670.

[5] B. Lipschultz, D. Whyte, and B. LaBombard, Plasma Phys. Control. Fusion **47** (2005) 1559.

[6] S.I. Krasheninnikov, Phys. Lett. A **283** (2001) 368.

[7] T.D. Rognlien, M.V. Umansky, X.Q. Xu, *et al.*, J. Nucl. Mater. **337-339** (2005) 327.

[8] A.Yu. Pigarov, S.I. Krasheninnikov, T.D. Rognlien *et al.*, Contrib. Plasma Phys. **44** (2004) 228.

[9] M. Kotschenreuther, T.D. Rognlien, and P. Valanju, Fusion Eng. Design **72** (2004) 169.

[10] T.D. Rognlien, D.D. Ryutov, N. Mattor, and G.D. Porter, Phys. Plasmas **6** (1999) 1851.

[11] D.P. Stotler, C.F.F. Karney *et al.*, Contrib. Plasma Phys. **40** (2000) 221; also http://w3.pppl.gov/degas2/.

[12] S.I. Braginskii, Transport processes in a plasma, *Reviews of Plasma Physics*, Vol. 1, Ed. M.A. Leontovich (Consultants Bureau, New York, 1965), p. 205.

**Figure captions**

(1) ITER geometry showing various magnetic flux surfaces and outer wall, with blow-ups of top secondary X-point region and lower primary X-point. Two magnetic separatrices are primary (short dashed line [red], $\psi = 1.0$) and secondary (long-dashed line [green], $\psi = 1.035$). Extended SOL between secondary separatrix and solid line (black, $\psi = 1.09$).

(2) Plasma radial velocity components are shown in (a) for the convective case ($V_c$ from Eq. 2), and b), the ion density with finite $V_c$ and $V_c = 0$, both at the outer midplane.

(3) In a), neutral density at the outer midplane with and without $V_c$, and b), radial ion flux at the wall ($\psi_m ax = 1.035$) versus poloidal distance moving closewise from the inner divertor.

(4) Ion density for radially extended domain ($\psi_m ax = 1.09$) in (a), with and without $V_c$ activated, and b), the corresponding electron temperature.

(5) Beryllium density and fluxes to the divertor plates.

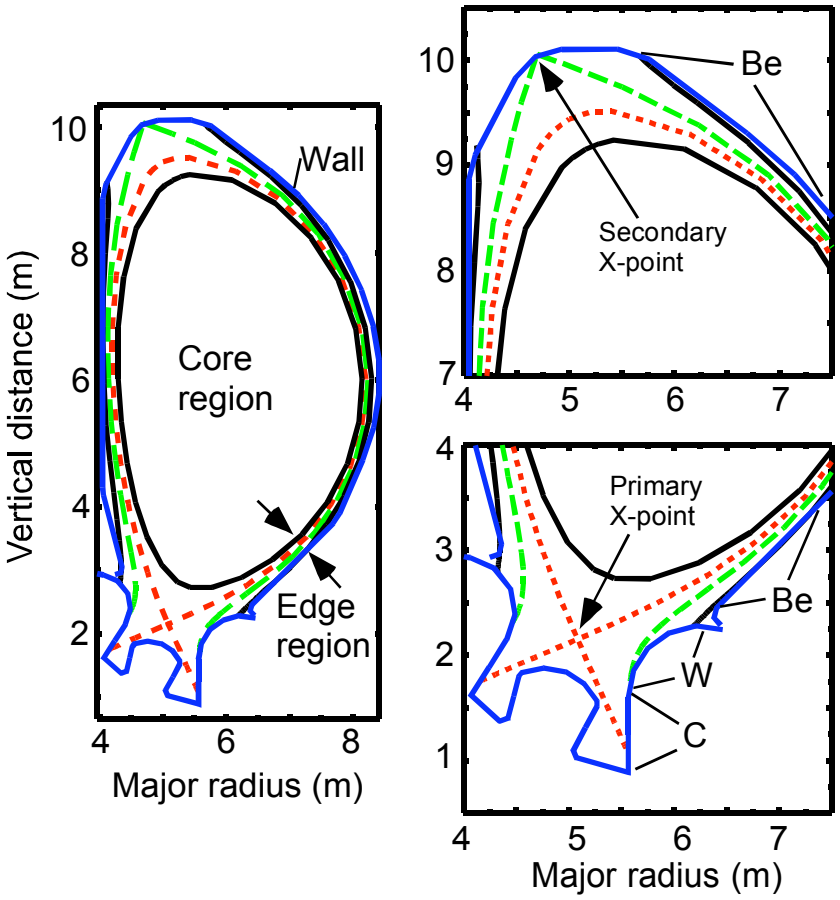
Vertical distance (m)
Major radius (m)
Wall
Core
region
Edge
region
Be
Secondary
X-point
Primary
X-point
Be
W
C
Major radius (m)

Fig. 1

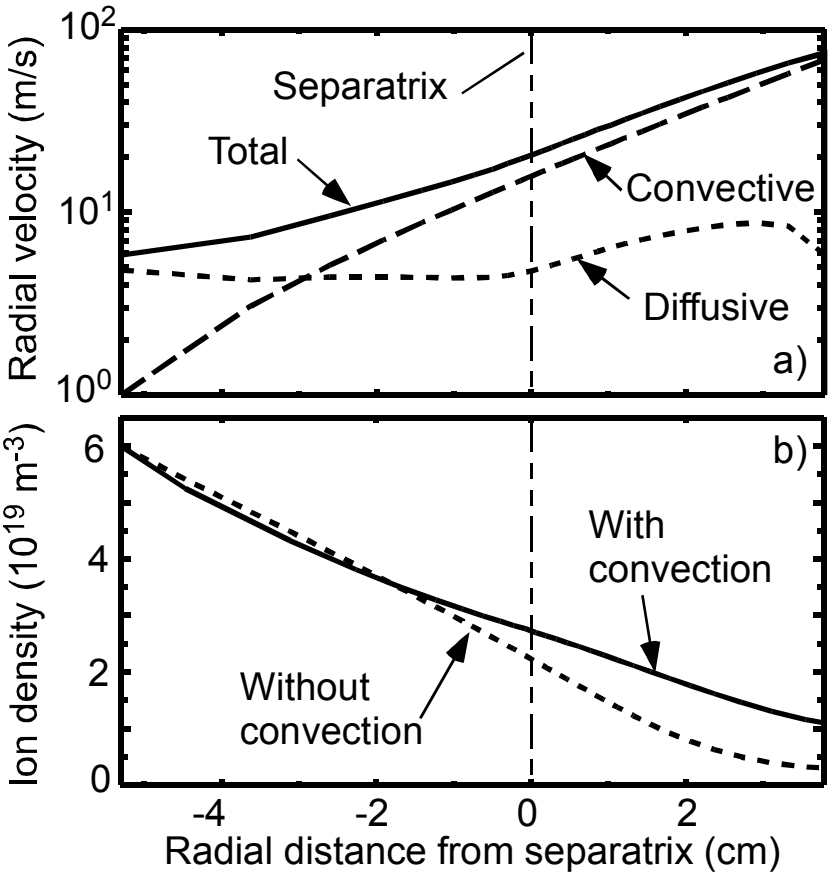
Radial velocity (m/s)
$10^2$
$10^1$
$10^0$
Separatrix
Total
Convective
Diffusive
a)
Ion density ($10^{19}$ $m^{-3}$)
6
4
2
0
b)
With convection
Without convection
-4
-2
0
2
Radial distance from separatrix (cm)

Fig. 2

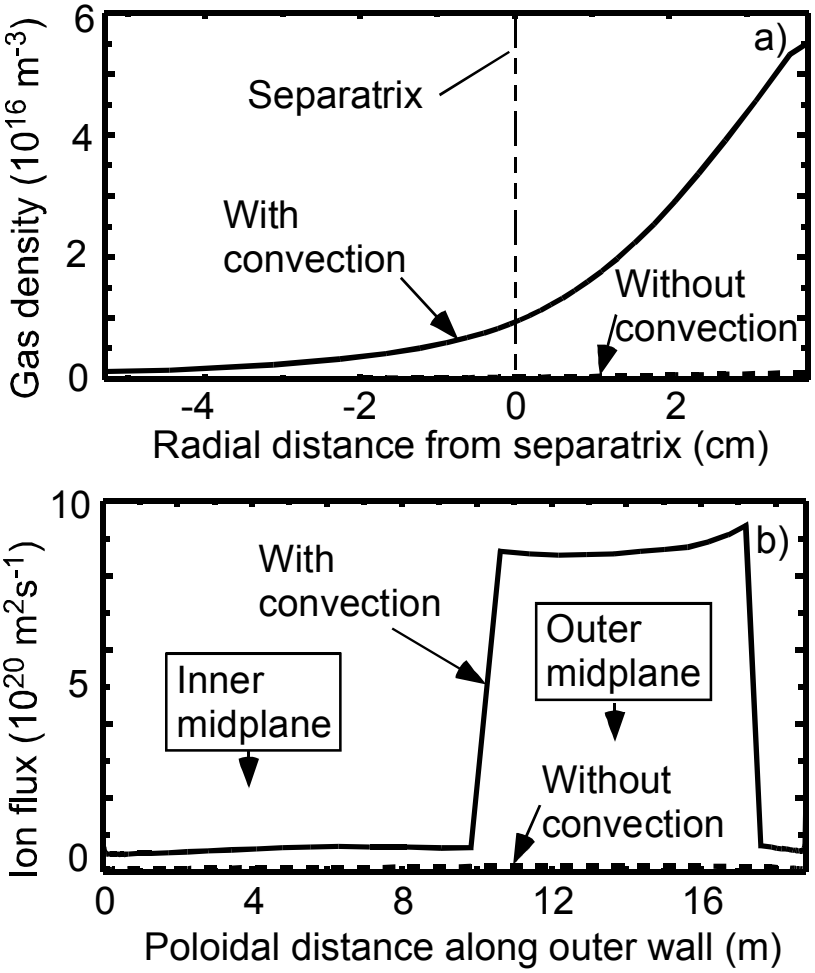
a)
Separatrix
With
convection
Without
convection
Gas density ($10^{16}$ m$^{-3}$)
Radial distance from separatrix (cm)
b)
With
convection
Inner
midplane
Outer
midplane
Without
convection
Ion flux ($10^{20}$ m$^{2}$s$^{-1}$)
Poloidal distance along outer wall (m)

Fig. 3

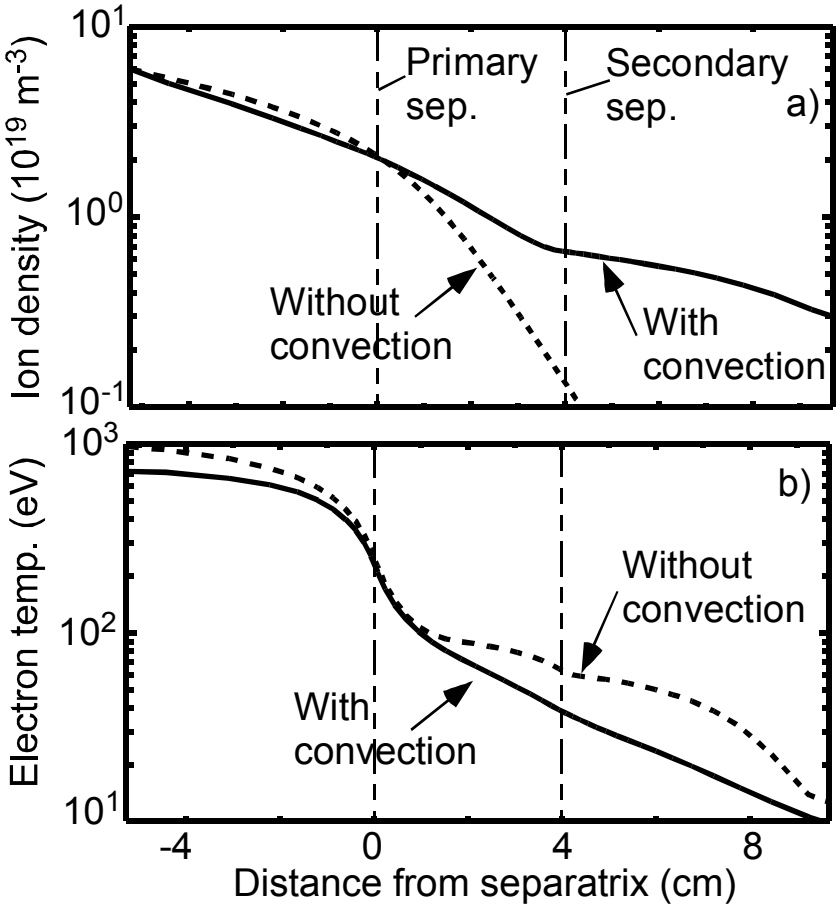
Ion density ($10^{19}$ $m^{-3}$)
$10^1$
$10^0$
$10^{-1}$
Primary sep.
Secondary sep.
a)
Without convection
With convection
Electron temp. (eV)
$10^3$
$10^2$
$10^1$
b)
Without convection
With convection
-4
0
4
8
Distance from separatrix (cm)

Fig. 4

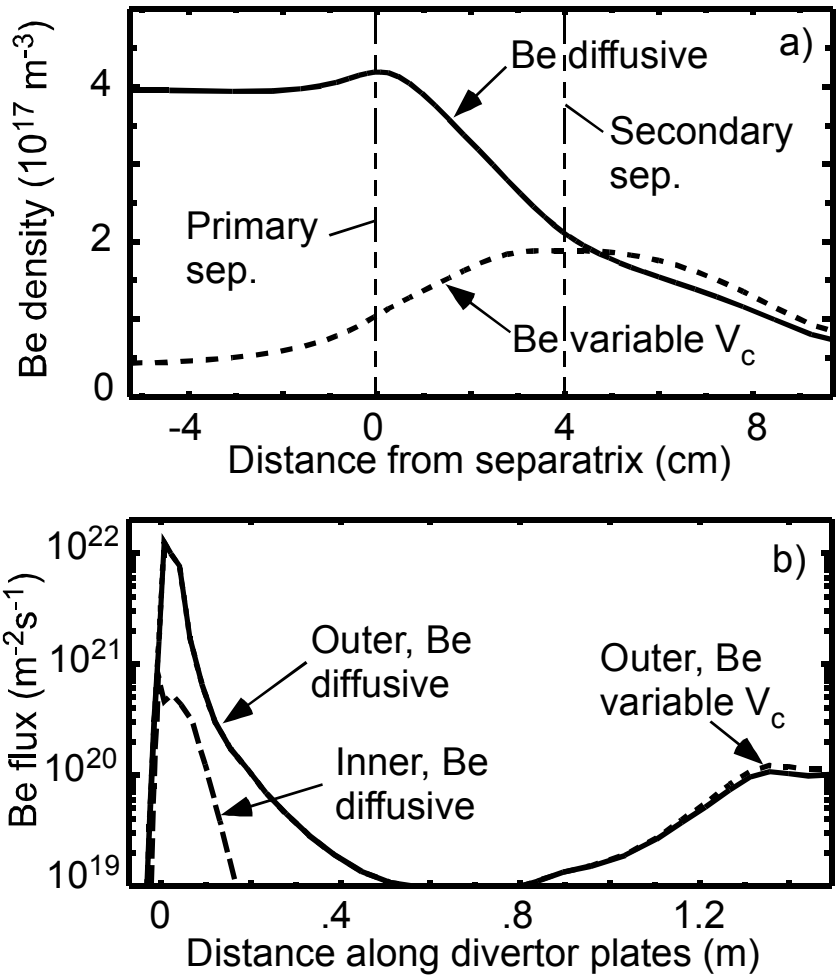
a)
Be diffusive
Secondary sep.
Primary sep.
Be variable $V_c$
Be density ($10^{17}$ $m^{-3}$)
4
2
0
-4
0
4
8
Distance from separatrix (cm)
b)
Outer, Be diffusive
Outer, Be variable $V_c$
Inner, Be diffusive
Be flux ($m^{-2}s^{-1}$)
$10^{22}$
$10^{21}$
$10^{20}$
$10^{19}$
0
.4
.8
1.2
Distance along divertor plates (m)

Fig. 5